Constant Potential Vorticity Hydraulically Controlled Flow—Complexities from Passage Shape*

J. A. WHITEHEAD

Department of Physical Oceanography, Woods Hole Oceanographic Institution, Woods Hole, Massachusetts

6 February 2002 and 2 August 2002

ABSTRACT

Velocity, surface height profiles, and volume flux are calculated for critically controlled flow of a layer of rotating fluid from a channel to an exit passage. The upstream fluid possesses constant potential vorticity. These are models of an internal layer of ocean water flowing out of a basin through a passage. An analysis is used that allows general passage bottom shapes. A number of features differ from those of nonrotating critically controlled flow. First, sizeable gyres appear for a range of upstream conditions. Second, more than one critical flow (maximum flux) is possible at the control point for the same upstream condition, but only one of these is allowed with continuous laminar flow from the channel to the passage. Third, a bottom that slopes away from the right-hand side (Northern Hemisphere rotation) and that is at right angles to flow direction produces small volume flux at high rotation rates. Fourth, although there is a rigorous bound for flux out of a passage, this is exceeded for some cases with multiple exits.

1. Introduction

Numerous problems have been studied in critical control of rotating fluid. For example, there are many cases developed in review articles by Griffiths (1986), Pratt and Lundberg (1991), Whitehead (1998), and Johnson and Clarke (2001) and examples in books (Pratt 1990). The typical calculation in such problems determines velocity and fluid surface profiles for flow through constricted passages in the presence of frame rotation. The fluid may attain a critical wave speed due to geometric changes along the flow path. At the point where flow is critical the shape of the passage controls flux magnitude. Problems are typically studied using theories that incorporate rotating fluid dynamics with idealized passage shapes. Frequently only one or two layers of fluids with different density are adopted due to the complicated nature of the algebraic solutions. Subsequent numerical studies using methods appropriate for transcritical flows can then clarify many aspects of temporal adjustment. In addition, constraints such as upper bounds have been found by replacing profiles determined by the equations of motion by profiles that extremalized some integral property of the flow (Killworth 1992, 1994; Killworth and McDonald 1993).

Probably the simplest possible configuration has inviscid rotating fluid with a free surface flowing out of a narrow passage from a big upstream reservoir. Rotation necessitates potential vorticity conservation. The first formulation assumed that zero potential vorticity fluid is supplied by the upstream fluid (Whitehead et al. 1974). The more general condition of upstream fluid with constant potential vorticity was soon analyzed (Gill 1977). This required a specification of both the nondimensional upstream potential vorticity and the ratio of volume flux between two upstream currents that lie in opposite walls of a very wide upstream channel. Using these two upstream conditions and information about the elevation of the exit passage bottom compared to upstream basin elevation, the velocity and surface elevation profiles are readily calculated.

If the passage bottom is not flat, the calculation is more challenging, because the ratio of volume flux between two currents in the upstream basin is not necessarily fixed as the bottom shape changes (Shen 1981). A recent thought experiment (Whitehead and Salzig 2001) motivates an alternative upstream condition to the ratio of volume flux. Consider an upstream channel of counterclockwise (Northern Hemisphere) rotating fluid of depth H initially at rest with respect to the rotating

* Woods Hole Oceanographic Institution Contribution Number 10767.

Corresponding author address: J. A. Whitehead, Department of Physical Oceanography, Woods Hole Oceanographic Institution, MS #21, Woods Hole, MA 02543-1541.
E-mail: jwhitehead@whoi.edu

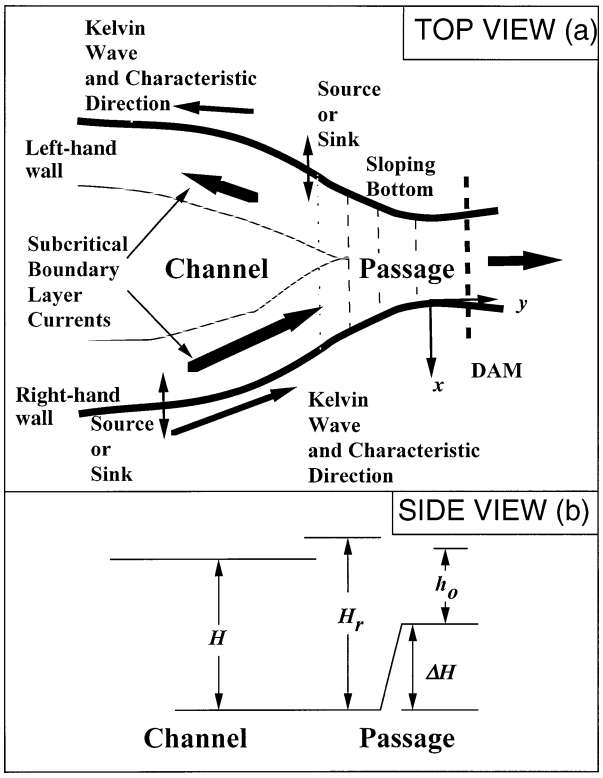

FIG. 1. (a) Plan view of the upstream channel and the passage. Waves transport information counterclockwise in the upstream channel so that no information from the left wall influences flow at the passage. (b) Elevation view of the channel and passage and definition of the change in bottom elevation and pertinent surface elevations.

frame as sketched in Fig. 1a (top panel). The upstream channel extent is infinite in the upstream direction, and its width is large compared to the Rossby radius of deformation. A gate is opened in a passage that removes fluid from the channel. A current is initiated by a wave of depression that propagates upstream from the passage along the left-hand wall of the channel. Note that all further references to right-and left-handed walls refer to the frame looking from the upstream channel to the passage. Gill (1976) describes the Kelvin wave on the left-hand wall in such a channel, and Pratt (1983, 1984) analyzes the characteristics. Specifically, if the current in the channel remains subcritical, the characteristic that conveys information upstream is trapped along the left-hand wall irrespective of currents that initially were in the channel before the exit flow starts. No current along the right-hand upstream wall is produced or altered by opening the passage. Then, additional currents can be started with pumps (of constant vorticity fluid) located in the walls of the channel. Using the characteristic solutions of Pratt (1983, 1984), it is readily shown that if the upstream depth is greater than zero everywhere in the channel, such wall currents are small enough to be subcritical with respect to the wave speed (Whitehead and Salzig 2001). For a wide channel, the characteristic signal for any newly formed current from the suddenly started source propagates to the right of the source looking offshore along the wall. Thus, the signal that sets up a current from either a source or sink on the left-hand wall of the channel moves away from the passage and does not influence the flow in the passage, as indicated in Fig. 1a. In contrast, the signal that sets up a current from either a source or sink lying along the right-hand wall of the channel propagates to the passage and influences the flow there.

This picture motivates a straightforward reformulation of the dynamics of nonlinear critically controlled rotating flow with constant potential vorticity following a path first explored by Shen (1981). We assert that the only upstream condition about currents required is the Bernoulli height along the streamline on the right-hand channel wall that extends to the passage. This condition applies downstream of all sources or sinks on the right-hand wall. As in all such problems, the well-known dynamical equations are the equation for geostrophic flow and the equation of constant potential vorticity. The latter requires a specification of depth of the fluid in the channel interior. This is a region that is away from the boundary currents in the wide upstream channel. The approach is similar to Gill's (1977) approach except that a different upstream Bernoulli condition is specified. There is no fundamental mathematical difference, but physically there is a difference. With this formulation, one can imagine that changing something at the passage will change the flow through the passage, but it does not change any physical upstream conditions that we set. These are the upstream fluid depth, the elevation of the passage floor above the floor of the upstream channel, and right-hand wall sources or sinks. In contrast, the earlier analysis held the ratio of the two upstream currents along the two sidewalls fixed without telling how this could be accomplished physically. The controlled flow at the passage was then calculated, and the two flows along the two walls in the upstream channel was then determined. The revised approach is at least of conceptual value.

This note presents a few results of such calculations. The objective is to show some effects peculiar to rotating fluid and thus to stimulate further work in conjunction with oceanographic, numerical, or advanced analytical work. The methods can easily be used to calculate results for other parameters.

2. Theory

Velocity distribution and fluid depth distribution across a constant potential vorticity current obey geostrophy and conservation of potential vorticity:

$$fv = g\frac{dh}{dx}, \tag{2.1a}$$

$$\frac{\dfrac{dv}{dx} + f}{h - b} = \frac{f}{H}. \tag{2.1b}$$

Here, $h(x)$ is elevation of the fluid surface, and $b(x)$ is elevation of the bottom above the deepest point in a controlling passage. A very wide channel lies upstream. H is the fluid depth in the middle of the channel far away from wall currents, f is the Coriolis parameter (positive for counterclockwise rotation), and g is the acceleration due to gravity (and we could consider this to be reduced gravity $g' = g\Delta\rho/\rho$ if we are studying a layer of fluid of density $\rho + \Delta\rho$, lying below an infinitely deep region of stagnant fluid of density ρ). A plan view of the channel and passage is shown in figure 1a along with the coordinates. The coordinate x is at right angles to the direction of flow, and v is velocity that is positive in the downstream direction. Gill (1977) showed that Bernoulli's equation is conserved along streamlines for this system, but that the upstream value of the Bernoulli function must be specified. We assume steady flow and utilize the Bernoulli function at the right-hand wall:

$$B = gH_r = \frac{1}{2}v^2 + g\bar{h}. \tag{2.2}$$

Here the overbar means that local height is the elevation above the upstream bottom. A streamline will extend from an upstream point on the right-hand upstream channel wall to the right hand wall in the passage. Using exponential solutions to Eqs. (2.1a,b) for the flow in the boundary currents in the channel, Whitehead and Salzig (2001) showed that Bernoulli height is

$$H_r = \frac{H}{2} + \frac{h_{ur}^2}{2H}, \tag{2.3}$$

where h_{ur} is surface elevation at the right-hand wall in the upstream channel. This elevation is related to the volume flux of the right-hand current $Q_r = g(h_{ur}^2 - H^2)/2f$. This flux is presumed to be known. In contrast, the current along the upstream left-hand channel wall is unknown and is set up by controlled flow in the passage. Figure 1b (bottom panel) shows an elevation view of some of the geometric and surface elevation parameters. At the passage, the deepest bottom point is ΔB above the upstream channel bottom and depth of the fluid in the passage at the right-hand wall (which we take as the origin) is h_0, so total surface elevation at the right-hand wall above the channel floor is $\bar{h} = h_0 + \Delta B$. Velocity there is found using (2.2) to be

$$v_0 = \sqrt{2g(H_r - \Delta B - h_0)}. \tag{2.4}$$

Using the following velocity, height, and lateral length scales, $\sqrt{g(H_r - \Delta B)}$, $H_r - \Delta B$, and $\sqrt{g(H_r - \Delta B)}/f$, Eqs. (2.1a,b) in the passage reduce to

$$\frac{dh'}{dx'} = v', \tag{2.5a}$$

$$\frac{dv'}{dx'} = [\zeta(h' - b')] - 1, \tag{2.5b}$$

where the primed are dimensionless variables. The dimensionless number $\zeta = (H_r - \Delta B)/H$ expresses the upstream condition. It is elevation of the Bernoulli height above the passage bottom divided by the potential vorticity height H [identical to $1 - \delta$ in Whitehead and Salzig (2001)] and it must be positive. In the passage, the boundary conditions are

$$h' = \gamma = h_0/(H_r - \Delta B), \tag{2.6a}$$

$$v' = v_0' = \sqrt{2(1 - \gamma)} \quad \text{at } x' = 0. \tag{2.6b}$$

We take flow out of the passage to be in the positive direction. Here γ is nondimensional height at the right-hand passage wall. This can take a wide range of values until some control condition is invoked. The axis for x is positive toward the right, so the integration from the right-hand wall must proceed in the negative x direction. In addition, other parameters could express the passage shape such as lateral width of the passage w, that is,

$$W = wf/\sqrt{g(H_r - \Delta H)}. \tag{2.7}$$

For any cross-passage bottom profile it is straightforward to pick values of the governing dimensionless parameters and numerically integrate (2.5a,b) across the passage. Volume flux is scaled by $g(H_r - \Delta H)^2/f$ and the maximum possible value of scaled flux through a passage is 0.5 (Killworth and McDonald 1993). This value corresponds to zero potential vorticity ($\zeta = 0$) flow over a wide flat passage (Whitehead et al. 1974). A critical condition is most easily found by calculating volume flux in the passage as a function of various values of γ and then finding γ_c, the value that produces a maximum volume flux. Gill (1977) showed that such maximized flow is also characterized by an arrested wave with Froude number equal to one.

3. Results

a. Upstream separation

As the water flows from a very deep upstream channel to a shallower passage, vortex columns shrink and vorticity of the fluid becomes negative. Vorticity amplitude can approach the dimensional value $-f$ for great contraction of vertical columns. This has the value -1 in dimensionless units. The resulting shear can produce stagnation along the right-hand wall (Shen 1981) and also sizeable recirculation upstream of the controlled flow (Borenas and Whitehead 1998). To demonstrate one effect of vertical contraction, some channel flow surface profiles have been calculated for the case with $\zeta = 0.01$. The results are shown in Fig. 2. At the top, above the bold line is a sketch of the profile in the very wide upstream channel that feeds fluid into the passage. The lateral coordinate for this profile is $x_u' = x_u/R'$ where $R' = \sqrt{gH}/f$ is Rossby radius based upon depth of the upstream fluid. Here we have assumed that the boundary current on the left-hand upstream wall supplies all the fluid. The bottom depth in the channel is -99 but all

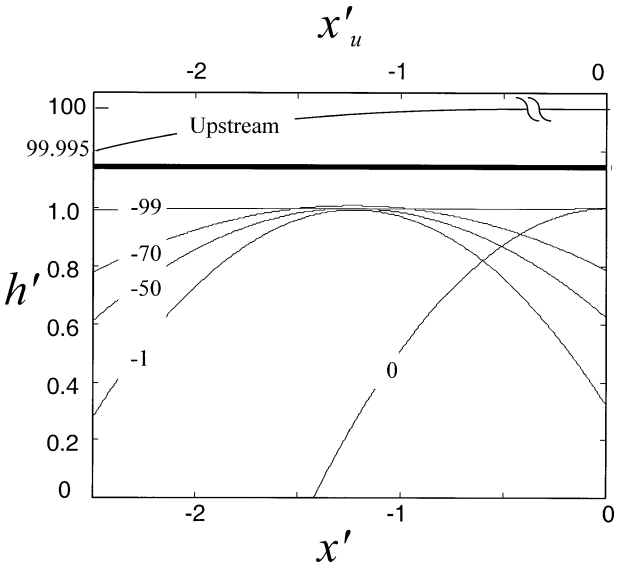

FIG. 2. Surface elevation profiles for flow approaching a flat passage for $\zeta = 0.01$. Above the bold line is sketched the height profile in the very wide upstream channel that feeds fluid into the passage. The lateral upstream channel coordinate is scaled by a Rossby radius based on the potential vorticity depth. Below the bold lines is shown surface height profiles in a passage of constant width approaching the control passage. Passage floor elevations are shown for the values $b = 0$, -1, -50, -70, and -99, respectively, which correspond to increasing depth as one progresses upstream from the control section to the deep upstream region. The parabolic profiles indicate the presence of a gyre upstream of the control passage.

channel bottom depths deeper than -50.0075 are possible as indicated in Eq. (2.19) of Whitehead and Salzig (2001). Different depths have different upstream current distributions.

The profiles in a narrow passage approaching the control passage are shown below the bold line. To calculate these profiles, Eqs. (2.5a,b) were integrated numerically across the passage starting from suitable initial conditions on the right-hand wall of the passage. The finite difference formulae were integrated starting from the right-hand wall in a negative direction. We used finite difference approximations to Eq. (2.1a,b) by setting $h'(m + 1) = h'(m) - v'(m)\delta x'$ and thereby finding surface elevations at point $m + 1$, and then by calculating velocity v' at that point with the formula $v'(m + 1) = v'(m) - \zeta[h'(m) - b(x')]\delta x' + \delta x'$. The step value $\delta x' = 0.001$ was used, and the equation was integrated 2500 steps across the passage. Consequently, scaled passage width is 2.5. The neglected terms are about $\delta x'^2/2$ plus higher order terms for each step. The estimate of our error across the opening is thus about 0.1%.

For the first calculations, elevation of the bottom of the passage was set to $b = 0$. The value of volume flux is $Q = \sum_{m=1}^{2500} [h'(m) - b(m)][v'(m)]\delta x'$. The maximum flux at the control passage is 0.5 with about 0.1% accuracy for $\gamma_c = 1$ as expected from earlier solutions to this problem. The value of shear ranges from -0.99 at the right hand wall to the value -1 at the point where the surface intersects the bottom. Therefore this flow has shear that approximates the value of -1 that corresponds to the dimensional value of $-f$ for zero potential vorticity (Whitehead et al. 1974) to about 1%. The profile of this surface appears to be almost perfectly parabolic.

To calculate the follows upstream, we took a narrow upstream channel with the same width as the controlled passage and in successive calculations set depth to the upstream values $b = -1$, -50, -70, and -99. The increasingly more negative values of b correspond to increasing passage depth with a constant width as one progresses upstream from the control section to the deep upstream channel region. We then altered γ by trial and error for each value of b to give $Q = 0.5$. For $b = -1$, -50, and -70, the calculations produced almost perfectly parabolic surface profiles that possessed significant negative surface elevation slope in the right-hand region. This signifies that there is a return flow in part of the passage, which in turn requires separation of the streamline from the upstream right-hand wall. The solution shows that streamlines for fluid flowing over the sill of the passage are located at the extreme left so that they have separated from the right-hand wall upstream of the passage. Values of shear in the regions approaching the controlled passage have values of approximately -0.98, -0.5, and -0.3 for each of the bottom depths of $b = -1$, -50, and -70, respectively.

Borenas and Whitehead (1998) noted the important feature that the local Bernoulli height in the recirculation region differs from any upstream value. These calculations illustrate this. For example, the surface elevation profile for $b = -70$ in Fig. 2 visibly extends above the level of the free surface ($h = 1$) in the upstream basin. This signifies that the Bernoulli function is greater than one for these streamlines. This differs from the model for zero potential vorticity where the Bernoulli function is one everywhere (Whitehead et al. 1974). A number of other differences between zero and very small potential vorticity are also shown by Borenas and Pratt (1994). For constant potential vorticity, the upstream Bernoulli function is only applied to the right-hand streamline of the fluid that leaves the region. It is easy to show that all fluid leaving the region has a Bernoulli function with value less than one as a consequence. Since the recirculation region is composed of fluid that does not leave the region between the wide upstream channel and the controlled passage, it can have a Bernoulli function greater than the value that is found along the upstream right-hand wall. Borenas and Whitehead (1998), analyze analytically upstream gyres in two-dimensional flows. Those examples do not contain such extreme shoaling of the bottom as are used in this example. Recirculation gyres are also prominent in their laboratory experiments and those by Whitehead and Salzig (2001).

Last, the surface height profile in the narrow upstream channel with the bottom elevation of -99 is also shown

in Fig. 2. This bottom elevation is the same as in the hypothetical infinitely wide upstream channel. Here, the surface profile has almost uniform slope and the change of surface elevation between the right-and left-hand wall is about 0.005. Shear is relatively small (<-0.005). There is no recirculation of the fluid and all of the fluid in this section flows up the slope and through the controlling passage. Thus the streamline along the right-hand wall detaches between this section and the one farther downstream.

It is readily shown that for $\zeta = 0.01$ any value of $b < -50.0075$ can provide a flux of 0.5 to the passage in the infinitely wide channel. The value $b = -50.0075$ is the highest bottom elevation that permits delivery of that amount of flux according to the relation of maximum upstream flux $Q_{\max} = (2r - 1)/\zeta^2$ according to Whitehead and Salzig [2001, their Eq. (2.19)]. Here $r = H_r/H$ is an additional dimensionless number that specifies the strength of the right-hand upstream current. Substitution of $b > -99$ produces $H_r < H$. This means that the flow along the right-hand channel wall is away from the passage and flow toward the passage is along the left-hand channel wall. For $b = -99$, $H_r = H$ and velocity is zero along the right-hand channel wall. This means that flow in the channel toward the passage is located only along the left-hand wall. For approximately $-99.1 < b < -99$ flow is toward the passage along both walls. For $b < -99.1$ flow is toward the passage along the right-hand wall and away from the passage along the left-hand wall. Regions upstream of oceanic sills may reasonably have parameters in the range $-99.1 < b < -99$, with currents along both walls flowing toward the passage and stagnant flow in the interior.

For b substantially above -99 the results seem bizarre for geophysical applications. The surface height of the stagnant fluid in the wide upstream channel interior is above one. For example, with $b = -50.0075$ (the highest bottom elevation possible), the stagnant interior surface height in the wide upstream channel is approximately 50. The water elevation along the left upstream channel wall is exactly $h_l = -50.0075$. An immense current with a flux of almost 5000 conveys water toward the passage along the left wall, and a slightly smaller current conveys water away from the passage along the right wall.

b. Multiple extrema

In contrast to all previous studies, multiple extrema have been found. To be specific, as the value of γ is smoothly changed downward from 1, the value of flux increases to a maximum value, then decreases to a minimum, then increases to a second maximum and then decreases again. These are found only with certain conditions present at the passage. First, the passage bottom shoals midway across the passage, it is deeper near the sides than at the center. Second, the multiple extrema are found only for $\zeta > 1$ so far. This condition requires either a shallow upstream channel or a sizeable current flowing toward the control section along the right-hand upstream wall (Whitehead and Salzig 2001).

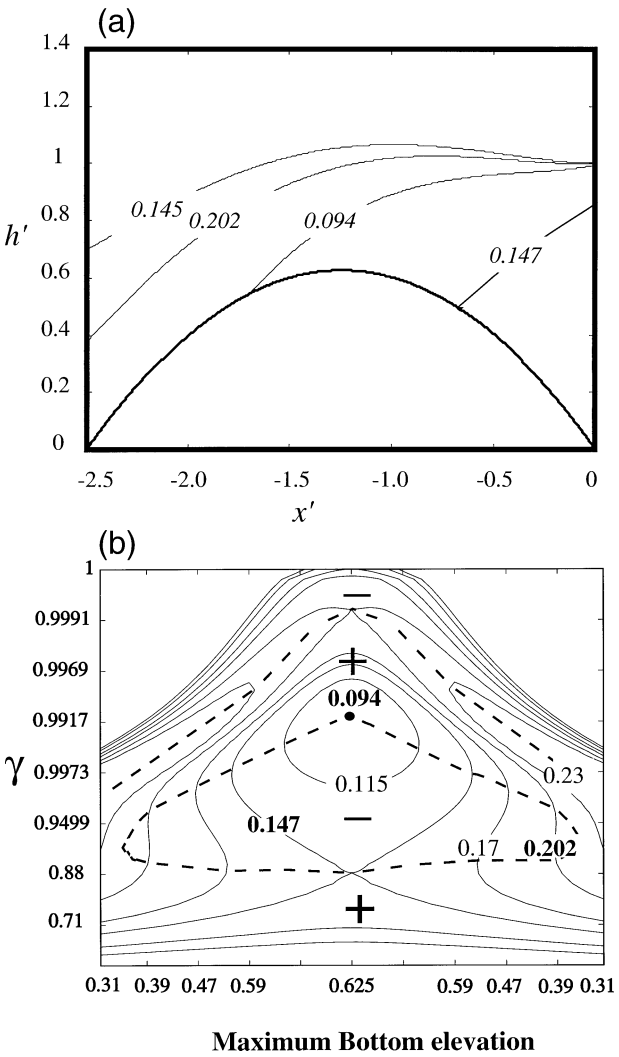

FIG. 3. (a) Surface height profiles over a parabolic bump across a passage for $\zeta = 1.5$ and $\gamma = 1.0$, 0.9993, 0.992, and 0.867, from top to bottom, respectively. Volume flux magnitude is given for each profile. The two volume flux maxima are shown by the second and fourth contours from the top. They are separated by the third contour for minimum flux. (b) Contours of volume flux as a function of the adjustable free parameter γ and elevation of the topography in the passage. The ordinate scale is nonlinear to stretch the values that are close to 1. The contours of the three critical values of flux from (a) are indicated by bold numbers. The two flux maxima possess the well-known crossing of iso-flow lines that characterize the connection of two conjugate states. The minimum is indicated by a point (enlarged for clarity). Other contours of flux are included to help visualization of the adjustment as the crest is approached. Their values are indicated by the other contour labels. The encircled pluses and minuses indicate regions where flow is either super- or subcritical, respectively; the four such regions being separated by the dashed curves.

An example of surface height profiles with multiple equilibria is illustrated in Fig. 3a. The bottom is a par-

abolic bump extending upward across the passage with an elevation of 0.625 above the deepest point. This example uses the value $\zeta = 1.5$. The volume flux as a function of γ contains two maxima separated by a minimum. The top curve shows the surface profile for $\gamma = 1.0$. For decreasing γ, volume flux increases until the first maximum is reached at $\gamma = 0.9993$, which is shown as the second profile from the top. The third profile is for minimum volume flux. Below this is the fourth profile, which possesses the second maximum volume flux.

The maximum and minimum volume fluxes in Fig. 3a are extrema (zero change in flux with a change in γ). Gill (1977) gave a simple explanation of why a flux extremum implies that there is a stationary wave. Essentially, the volume flux is unchanged with a change in surface elevation so that a wave is frozen in position. Therefore, all three extrema in Fig. 3a are consistent with a stationary wave in the passage.

Figure 3b illustrates the adjustment of some of the flow parameters as the crest of the bottom is approached and passed. Parameters are the same as in Fig. 3a. Selected contours of volume flux are shown as a function of h_0 and elevation of the bottom. The contours of the three critical values of flux are shown. The two flux maxima possess the well-known crossing of iso-flow lines that characterize the connection of two conjugate states. The minimum is indicated by a point (enlarged for clarity). Some other contours of flux are included to help visualization of the adjustment as the crest is approached. The pluses and minuses indicate regions where we infer that flow is either super or subcritical, respectively; the four such regions are separated by the dashed curves.

Figure 3b indicates that the middle subcritical region does not extend far upstream and downstream of the bottom crest. The consequence is that the lower maximum contours are not connected with a conjugate state at the other end of the channel. One must conclude that even though Fig. 3a indicates the possibility of multiple equilibria in the form of two maxima and one minimum, the lower maximum and the minimum in flux cannot be realized by continuous laminar flow from upstream of the passage to downstream. This also means that setting the Froude number equal to one in the control section generates some flows that cannot continuously flow through the passage.

The profile for the top maximum has a small region of flow reversal for the critically controlled flow. Borenas and Lundberg (1986) also found some maxima with flow reversal over a differently shaped parabolic bottom (with greatest depth at the center). Since the gyre in such a region will gradually slow down due to any small amount of friction, the nature of control in such problems is still not clearly understood.

c. Limitations from bottom slope

If the bottom slopes away from the right-hand wall, a sufficiently small bottom slope limits the cross-stream surface slope and thereby by Eq. (2.1a) prevents large velocities. This can produce small values of flux even if the opening is very wide. Figure 3 shows the surface height profiles for a passage with a bottom uniformly sloping away from the right-hand side. Three different values of scaled passage width are shown. For all three cases maximum flux is found for $\gamma = 1$. The top profile has $W = 0.675$. The value of critical (maximum) flux is 0.076. The middle profile has $W = 1.25$. The interface adopts a slope very close to that of the bottom slope, and the volume flux is 0.210. This is a value much larger than the top profile but still less than the maximum bound of 0.5. The bottom profile has $W = 1.875$. The current is confined to a layer along the upper part of the slope and volume flux is 0.066. Essentially, flux is limited because the fluid velocity cannot exceed a value dictated by the slope of the bottom over a sizeable region. Thus, with a bottom sloping away from the right-hand wall, there is an opening width that admits greatest flux. Both narrower and wider openings admit less flux. These results were for $\zeta = 1.0$. Calculations with other values gave very little qualitative difference.

Borenas and Lundberg (1986) found that volume flux becomes very small in a very wide passage with a parabolic bottom with depression in the middle (rather than elevation as in Fig. 2). The bottom was intended to be a first approximation to smoothly varying ocean passages. They found that currents with unidirectional flow were confined to a narrow boundary current along the right-hand sloping bottom. These narrow currents did not have maximum volume flux. Instead, currents extending over a sizeable portion of the passage had the most volume flux, but these had very large return flows. Shen (1981) also explored this problem but only found an increase of flux with rotation. The analysis did not extend to the asymptotic large rotation limit we show next.

The analytical solution for the flux of zero potential vorticity fluid ($\zeta = 0$) through a passage like that sketched in Fig. 4 is $Q = (8/3W^3)(1 + 3/4W)$ with $\gamma_c = 1$. It is valid for $W \geq 2$. Our numerical calculations produced similar results with $Q \sim W^{-3}$ for large width and over a wide range of ζ.

d. Interrupted passages

With two passages with flat bottoms, flux can exceed the maximum possible flux for one passage. It was shown that the upper bound of flux through a single passage for all upstream values of vorticity and for all passage bottom shapes is 0.5 (Killworth and McDonald 1993). Since the Bernoulli function is almost the same for all streamlines in the limit of a very deep upstream passage (which approaches the zero potential vorticity limit), it is easy to exceed this maximum flux with two passages, especially with $\zeta \approx 0$. For example, Fig. 5 shows a calculation with $\zeta = 0.1$ where the two passages produce a total maximum flux of 0.931. Profiles have

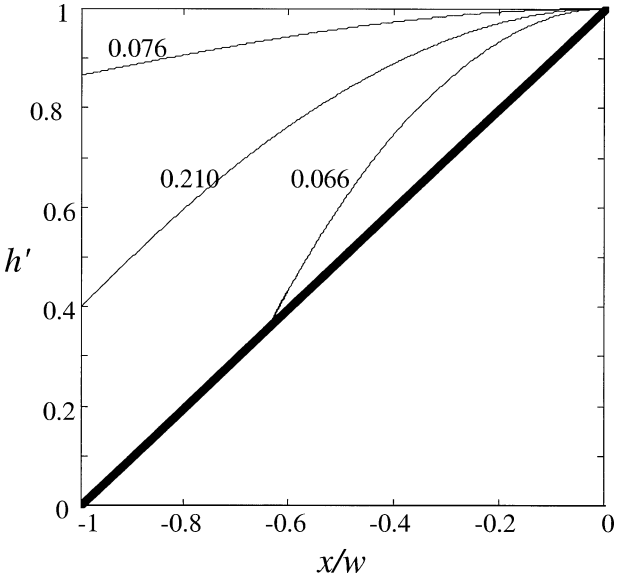

FIG. 4. Three surface profiles and their associated values of volume flux for cases with a narrow, moderate, and wide channel, respectively. The top curve has $W = 0.675$, the middle has $W = 1.25$, and the bottom has $W = 1.875$.

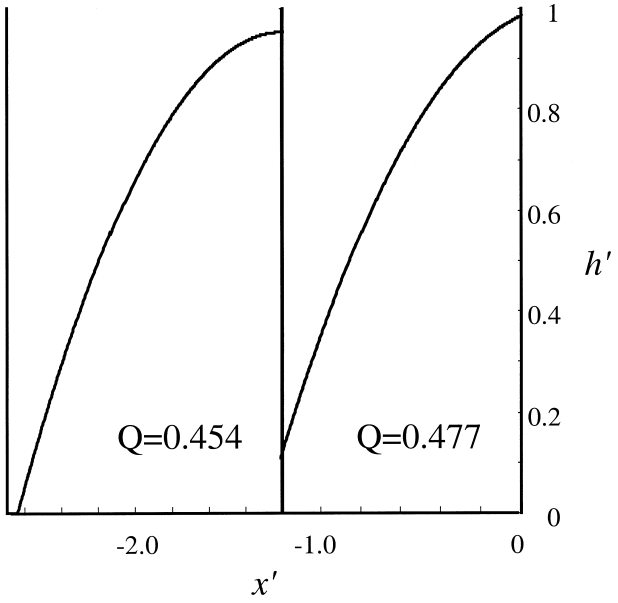

FIG. 5. Two passages with flat bottoms for $\zeta = 0.1$. The maximum flux was found first for the right-hand channel and then the flux in the left-hand channel was maximized keeping the same value of Bernoulli height on both sides of the middle wall. Combined flux of the pair has more flux than the upper bound for a single passage.

been calculated upstream as in section 3a, as well. Each passage develops a parabolic surface that indicates a return flow. This implies that a gyre is found for increasingly negative b until at $b = -9.0$ the gyre vanishes. The two surfaces lose their region of negative slope and merge into a unidirectional upstream flow. Streamlines on both sides of the middle wall have the same elevation and slope. The wall can vanish at that bottom elevation. Anywhere upstream the channel can be widened indefinitely. Calculations reveal that the total maximum flux for two passages with flat bottoms goes down with increasing ζ. For example, with $\zeta = 1$, the total maximum flux for both passages is only 0.58.

There are also peculiar results which seem physically unimportant but which may warrant further study. For example, with $\zeta > 1$ the flux can be indefinitely big for two passages if reverse flow is allowed in the right-hand passage and the wall dividing the two passages extends above $b = 1$. In that case, the Bernoulli height at the dividing passage can be larger than one, and the left-hand passage can have very large, and even perhaps indefinitely large flux. Most such fluid streamlines originate downstream of the controlled passage because such a Bernoulli height does not exist in the upstream channel. Therefore, this result seems to be badly posed physically. Further investigation into all the features of multiple outlets is needed to understand such surprising results.

4. Implications of the results

This note illustrates new effects of passage bottom configuration. These new features are revealed without studying them in exhaustive detail. We indicate simple methods for further computation.

First is the possibility of a passage containing a Bernoulli potential greater than the upstream value for fluid that has a return flow in the passage. This happens because the streamlines in closed gyres do not originate in the upstream region.

The second is that there can be more than one local flux maximum. The results seem most pronounced for $\zeta > 1$. The presence of more than one extremum implies that there is more than one condition with an arrested wave. However, calculations in the upstream regions show that only one extremum is physically realized.

The third new effect is the limitation of flow by passage floors that tilt away from the right-hand fluid surface with small angles. Some passages in the ocean may be sufficiently smooth to limit flow velocity in this way, a possibility already raised by Borenas and Lundberg (1986). One intriguing possibility is that viscous flux in the bottom boundary layer under such currents may alter the hydrodynamic conditions of the flow in such a way that greater flux is achieved with friction than without. This is only conjectural at this point, but the manner in which Borenas and Lundberg (1986) found that the greatest flux is achieved for flows with closed gyres suggests that masses of stagnant water might act as artificial walls that enhance flows above gradually sloping bottoms.

The fourth new effect is that flux out of passages can exceed the value given by upper bounding theory. How-

ever, this is due to multiple passages, and thus it is not formally covered by existing theories.

Since both the second and forth effects involve the deflection and even splitting of streamlines by topography, this seems to be an area for further study. In no case has a comprehensive exploration of parameter space been conducted for these new effects. The method used here is sufficiently simple that further calculations of this sort in a number of directions are possible. By using more advanced methods, a number of questions could be answered. For example, a complete understanding of the time adjustment in the manner developed for simple bottom topography (Pratt 1983, 1984) would be very useful, as would numerical studies. Particularly important are the properties of information propagation with multiple outlets.

In planning future projects in the oceans to measure flux through passages that appear to control flow, calculations like these can help to decide on the best location of measurements. These results illustrate the importance of the Bernoulli height upstream of the passage along the right-hand channel wall whereas existing analyses (Whitehead 1989, 1998) only utilize this height in the interior. These results also indicate that careful placement of measurements is vital. Obviously one current meter inside a gyre might measure a flow that is in the direction opposite to the mean flow direction. In addition, any currents approaching along the right-hand upstream wall must be included in estimating the Bernoulli elevations. Indeed, the location of currents that feed the ocean overflows are unknown, and we hope that these and future calculations might help to clarify their role more clearly.

Acknowledgments. Support was provided by The National Science Foundation, Physical Oceanography section, under Grant OCE0081179.

REFERENCES

Borenas, K., and P. Lundberg, 1986: Rotating hydraulics of flow in a parabolic channel. *J. Fluid Mech.,* **167,** 309–326.

——, and L. J. Pratt, 1994: On the use of rotating hydraulic models. *J. Phys. Oceanogr.,* **24,** 108–123.

——, and J. A. Whitehead, 1998: Upstream separation in a rotating channel flow. *J. Geophys. Res.,* **103** (C4), 7567–7578.

Gill, A. E., 1976: Adjustment under gravity in a rotating channel. *J. Fluid Mech.,* **77,** 603–621.

——, 1977: The hydraulics of rotating channel flow. *J. Fluid Mech.,* **80,** 641–671.

Griffiths, R. W., 1986: Gravity currents in rotating systems. *Annu. Rev. Fluid Mech.,* **18,** 59–89.

Johnson, E. R., and S. R. Clarke, 2001: Rossby wave hydraulics. *Annu. Rev. Fluid Mech.,* **33,** 207–230.

Killworth, P. D., 1992: Flow properties in rotating, stratified hydraulics. *J. Phys. Oceanogr.,* **22,** 997–1017.

——, 1994: On reduced-gravity flow through sills. *Geophys. Astrophys. Fluid Dyn.,* **75,** 91–106.

——, and N. R. McDonald, 1993: Maximal reduced-gravity flux in rotating hydraulics. *Geophys. Astrophys. Fluid Dyn.,* **70,** 31–40.

Pratt, L. J., 1983: On inertial flow over topography. Part 1. Semigeostrophic adjustment to an obstacle. *J. Fluid Mech.,* **131,** 195–218.

——, 1984: On inertial flow over topography. Part 2. Rotating channel flow near the critical speed. *J. Fluid Mech.,* **145,** 95–110.

——, 1990: *The Physical Oceanography of Sea Straits.* NATO ASI series, Vol. 318, Kluwer Academic, 587 pp.

——, and P. A. Lundberg, 1991: Hydraulics of rotating strait and sill flow. *Annu. Rev. Fluid Mech.,* **23,** 81–106.

Shen, C. Y., 1981: The rotating hydraulics of the open-channel flow between two basins. *J. Fluid Mech.,* **112,** 161–188.

Whitehead, J. A., 1989: Internal hydraulic control in rotating fluids—Applications to oceans. *Geophys. Astrophys. Fluid Dyn.,* **48,** 169–192.

——, 1998: Topographic control of ocean flows in deep passages and straits. *Rev. Geophys.,* **36,** 423–440.

——, and J. Salzig, 2001: Rotating channel flow: Control and upstream currents. *Geophys. Astrophys. Fluid Dyn.,* **95,** 185–226.

——, A. Leetmaa, and R. A. Knox, 1974: Rotating hydraulics of strait and sill flows. *Geophys. Fluid Dyn.,* **6,** 101–125.